

CuIn_{1-x}Ga_xSe₂ Thin Film Solar Cells

**Final Subcontract Report
5 January 1998—31 October 2001**

N.G. Dhere
*Florida Solar Energy Center
Cocoa, Florida*



NREL

National Renewable Energy Laboratory

1617 Cole Boulevard
Golden, Colorado 80401-3393

NREL is a U.S. Department of Energy Laboratory
Operated by Midwest Research Institute • Battelle • Bechtel

Contract No. DE-AC36-99-GO10337

CuIn_{1-x}Ga_xSe₂ Thin Film Solar Cells

**Final Subcontract Report
5 January 1998—31 October 2001**

N.G. Dhere
*Florida Solar Energy Center
University of Central Florida
Cocoa, Florida*

NREL Technical Monitor: B. von Roedern

Prepared under Subcontract No. XAK-8-17619-12



NREL

National Renewable Energy Laboratory

1617 Cole Boulevard
Golden, Colorado 80401-3393

NREL is a U.S. Department of Energy Laboratory
Operated by Midwest Research Institute • Battelle • Bechtel

Contract No. DE-AC36-99-GO10337

NOTICE

This report was prepared as an account of work sponsored by an agency of the United States government. Neither the United States government nor any agency thereof, nor any of their employees, makes any warranty, express or implied, or assumes any legal liability or responsibility for the accuracy, completeness, or usefulness of any information, apparatus, product, or process disclosed, or represents that its use would not infringe privately owned rights. Reference herein to any specific commercial product, process, or service by trade name, trademark, manufacturer, or otherwise does not necessarily constitute or imply its endorsement, recommendation, or favoring by the United States government or any agency thereof. The views and opinions of authors expressed herein do not necessarily state or reflect those of the United States government or any agency thereof.

Available electronically at <http://www.doe.gov/bridge>

Available for a processing fee to U.S. Department of Energy
and its contractors, in paper, from:

U.S. Department of Energy
Office of Scientific and Technical Information
P.O. Box 62
Oak Ridge, TN 37831-0062
phone: 865.576.8401
fax: 865.576.5728
email: reports@adonis.osti.gov

Available for sale to the public, in paper, from:

U.S. Department of Commerce
National Technical Information Service
5285 Port Royal Road
Springfield, VA 22161
phone: 800.553.6847
fax: 703.605.6900
email: orders@ntis.fedworld.gov
online ordering: <http://www.ntis.gov/ordering.htm>



Contents

CuIn _{1-x} Ga _x Se ₂ Thin Film Solar Cells	1
1. Introduction	1
2. CIGS ₂ Thin Film Solar Cells on Stainless Steel Foils	1
3. Large-Area, Dual-Chamber Magnetron-Sputtering Unit	3
4. Round Robin AES and SIMS Analysis	3
5. IxV Characteristics of CdTe Modules and Analysis of CdTe Module Samples	4
Appendix 1: CIGS ₂ Thin Film Solar Cells on Stainless Steel Foil (Reproduced with permission from MRS)	H3.4.1
Abstract	H3.4.1
1. Introduction	H3.4.1
2. Experimental Technique	H3.4.2
3. Results and Discussions	H3.4.3
4. Conclusions	H3.4.6
References	H3.4.6
Appendix 2: Large-Area, Dual-Chamber Magnetron-Sputtering Unit for Preparation of CIGS Thin Film Solar Cells (2001 NCPV Program Review Meeting)	A2-1
Abstract	A2-1
1. Introduction	A2-1
2. Experimental Technique	A2-2
3. Round Robin AES and SIMS Analysis	A2-2
4. IxV Characteristics of CdTe Modules	A2-2
5. Results and Discussions	A2-2
References	A2-2
Appendix 3: Lightweight CIGS ₂ Thin-Film Solar Cells on Stainless Steel Foil (Reproduced with permission from WIM-Munich)	A3-1
1. Introduction	A3-1
2. Experimental Technique	A3-1
3. Results and Discussions	A3-1
4. Conclusions	A3-4
References	A3-4

CuIn_{1-x}Ga_xSe₂ Thin Film Solar Cells

1. Introduction

This is the final report of the NREL project entitled, “CuIn_{1-x}Ga_xSe₂ Thin Film Solar Cells”, NREL contract no. XAK-8-17619-12, UCF/FSEC Account no. 26-58-810. It briefly describes the development of CIGS2 thin film solar cells on stainless steel foils, fabrication of a large-area, dual-chamber magnetron-sputtering unit, Round Robin AES and SIMS analysis, and IxV characteristics of CdTe modules and Analysis of CdTe Module Samples. More detailed results on CIGS2 cells and large-area dual-chamber magnetron-sputtering unit presented at the MRS Conference and being presented at the European PV Conference and NCPV Program Review Meeting are included in the Appendices I, II and III. The results of Round Robin AES and SIMS analysis are being submitted to the National CIGS Team Meeting while the IxV characteristics of CdTe modules and results of analysis of CdTe Module Samples are being submitted separately to NREL and First Solar.

Four Graduate students, Mr. Shashank R. Kulkarni, Mr. Sanjay S. Chavan, Shantinath R. Ghongadi, and Mandar B. Pandit successfully defended M.S. theses based on the research carried out at FSEC PV Materials Lab.

2. CIGS2 Thin Film Solar Cells on Stainless Steel Foils

DC sputter-deposition parameters of molybdenum back-contact layer from 3” diameter magnetron sputtering source were optimized so as to minimize the residual stresses developed during deposition. Depending on the working gas pressure, residual stresses can develop in refractory metal thin films prepared by magnetron sputtering. Films deposited below a transition pressure are in compression whereas those deposited above the transition pressure develop tensile stress. It is believed that such stress reversal is dependent on energetic bombardment by reflected neutrals and/or sputtered atoms. At relatively low pressures, the arriving atoms have higher kinetic energy and the resulting film has dense microstructure but at the same time experiences compressive stress. A higher working gas pressure is expected to moderate the flux and energy of these particles and consequently form a more open morphology with a tensile stress. The adhesional strength at the Mo/stainless steel substrate was tested using a simple scotch tape test to gauge the tendency of the films to peel off due to excessive residual stresses. Sheet resistance was measured with two-probe resistance measurement. Composite Mo back contact films prepared by alternatively depositing three layers at high argon pressure of 9 mTorr and low power of 40 W, and three layers deposited at low argon pressure on 5 mTorr and high power of 70 W demonstrated good adhesion and very low sheet resistance.

Bright annealed stainless steel (SS) foils of thicknesses 127 μm and 20 μm were evaluated as possible substrate materials for polycrystalline CIGS2 solar cell.

Approximately 40%-Cu-rich Cu-Ga/In layers were sputter-deposited on unheated Mo-coated SS foils from CuGa(22%) and In targets. Well-adherent, large-grain Cu-rich CIGS2 films were obtained by sulfurization in a Ar:H₂S 1:0.04 mixture and argon flow rate of 650 sccm, at the maximum temperature of 475° C for 60 minutes with an intermediate 30 minute annealing step at 135° C. p-type CIGS2 thin films were obtained by etching away the Cu-rich layer segregated at the surface in dilute KCN solution.

The chemical composition of CIGS2 films was analyzed by electron-probe microanalysis (EPMA), Auger electron spectroscopy (AES) and secondary ion mass spectrometry (SIMS) depth profiling by positive SIMS using CAMECA IMS-3F system with oxygen primary beam current of 150 nA, impact energy of 5.5 keV, angle of incidence of 42° , rastered over a $250\text{ }\mu\text{m} \times 250\text{ }\mu\text{m}$ area, with source at 10 keV and sample at 4.5 keV. Structure and morphology of CIGS2 films was studied by X-ray diffraction (XRD) and scanning electron microscopy (SEM).

Solar cells were completed by deposition of CdS heterojunction partner layer by chemical bath deposition, transparent-conducting ZnO/ZnO:Al window bilayer by RF sputtering, and vacuum deposition of Ni/Al contact fingers through metal mask. PV parameters of a solar cell on SS foil were measured under AM 1.5 and AM 0 illumination respectively at National Renewable Energy Laboratory (NREL) and NASA Glenn Research Center (NASA GRC). Detailed PV characteristics were obtained at the Institute of Energy Conversion (IEC).

Once the Cu-excess in CIGS2 films was optimized, uniform, bluish gray CIGS thin films were obtained on flexible SS foils. The two probe method showed very low resistance indicating that the film was copper rich and Cu_{2-x}S phase had segregated uniformly on the surface.

Average atomic concentrations of Cu:In:Ga:S proportion of 24.83:22.96:2.07:50.14 measured by EPMA in CIGS2 films on SS foils at incident electron beam energy of 20 keV. This is equivalent to CIGS2 compound formula of $\text{Cu}_{0.99}\text{In}_{0.92}\text{Ga}_{0.08}\text{S}_2$. At incident electron beam energy of 10 keV, the proportion of gallium was lower due to the tendency of gallium to diffuse towards the back contact. In an unetched Cu-rich CIGS2 film, proportion of atomic concentration of Cu:In:Ga:S as measured by EPMA at 20 keV was 41.55:13.41:1.09:43.963.

SIMS depth profile for the etched sample showed uniform sulfur signal throughout the entire thickness. Gallium signal strength increased slightly while indium signal strength decreased at larger depths. The increase in copper signal strength at higher depths was probably an artifact of film roughness. Potassium incorporation in the film was due to etching with KCN solution. Sodium was not intentionally added and also the samples were handled with extreme care using tweezers. Even then small amounts of sodium were detected in the film.

SEM image of an unetched CIGS2 thin film on SS foil substrates showed large ($\sim 3\text{ }\mu\text{m}$ size), compactly packed, faceted grains. Besides the 110 peak from molybdenum, XRD pattern for the etched CIGS2 film on SS foil showed the following reflections from the chalcopyrite CIGS2 phase with $a_0 = 5.519\text{ }\text{\AA}$ and $c_0 = 11.125\text{ }\text{\AA}$: 101, 112, 103, 200, 211, 220, 213, 312, 322, 400, and 332. Reflection 112 was proportionately stronger compared to that in the standard powder pattern. Thus the CIGS2 film grew with $\{112\}$ preferred orientation.

PV parameters of a CIGS2 solar cell on $127\text{ }\mu\text{m}$ thick SS flexible foil measured under AM 1.5 conditions at NREL were as follows: $V_{oc} = 788\text{ mV}$, $J_{sc} = 19.78\text{ mA/cm}^2$, $FF = 59.44\%$, $\eta = 9.26\%$. For this cell, the AM 0 PV parameters measured at NASA GRC were as follows: $V_{oc} = 802.9\text{ mV}$, $J_{sc} = 25.07\text{ mA/cm}^2$, $FF = 60.06\%$, and $\eta = 8.84\%$. Preliminary experiments were carried out for preparation of CIGS2 cells on $20\text{ }\mu\text{m}$ thick SS foils. Low 4.06% (AM 1.5) efficiency of an un-optimized CIGS2 solar cell on $20\text{ }\mu\text{m}$ thick SS foil is attributed to higher foil roughness.

Detailed consisting of the analysis of short circuit current, J versus voltage, V gave values of series resistance R_s , shunt resistance R_p , diode factor A, and reverse saturation current J_0 , of $\sim 0.1\text{ }\Omega\text{ cm}^2$, $\sim 600\text{ }\Omega\text{ cm}^2$, ~ 2.2 and $\sim 1.85 \times 10^{-8}\text{ A cm}^{-2}$ respectively.

Quantum efficiency (QE) curves were obtained in the dark and under AM1 light illumination, without bias ($V = 0$) and with reverse (-0.5 V) and forward (0.5 V) bias. They showed only a modest loss at high energy by the thin heterojunction partner CdS layer. At low

energy, a sharp QE cutoff was observed equivalent to CIGS2 bandgap of ~ 1.50 eV. This is fairly close to the required optimum value for efficient AM0 PV conversion in the space.

Overall the detailed PV characterization consisting of J-V analysis and quantum efficiency data showed that CIGS2 thin film solar cells on 127 μm thick SS substrates were normal without serious limitations.

3. Large-Area, Dual-Chamber Magnetron-Sputtering Unit

During the last eleven years, FSEC PV Materials Laboratory has established facilities for magnetron sputter deposition of molybdenum back contact layer and CuGa/In metallic precursor layers, selenization and sulfurization of metallic precursors, CdS chemical bath deposition, and ZnO/ZnO:Al RF sputter deposition. Earlier, the substrate size was limited to 1" x 1". A large-area, dual-chamber magnetron-sputtering unit has been fabricated recently. Both the chambers are equipped with cryopumps, two-stage mechanical vacuum pumps, throttled-gate valves, mass-flow controllers for argon and oxygen, and convectron and Bayard-Alpert ionization gauges. A large number of feed-thru ports have been provided to both the chambers for rotation and electrical feed-thru's. This will permit addition of *in situ* diagnostic tools.

The large chamber has three 4" x 12" DC magnetron sputtering sources for sputter deposition from molybdenum, indium, and copper, CuGa (22%) or CuGa (67%) targets. A linear substrate movement set-up has been fabricated for "in line" deposition of molybdenum back contact and Cu-Ga/In metallic precursors. Presently the movement of the substrates is carried out manually. Precise movement using stepper motor will be carried out in the near future.

The small chamber has two 4" x 12" RF magnetron sputtering sources, installed for RF sputter deposition from ZnO and ZnO:Al targets.

The thickness uniformity along the 12" dimension is expected to be better than $\pm 2\%$ over the center width of 5" and better than $\pm 3\%$ over the center width of 6" for linear substrates motion along the 4" dimension. Moreover, the sputtering sources are expected to provide excellent ($>40\%$) target utilization. A four-hearth e-beam source has also been procured for vacuum evaporation of Ni/Al contact grids. The vacuum chambers were designed at FSEC and were built elsewhere based on FSEC design. The complete system was designed and constructed at FSEC. Several Graduate students have been trained in the design and construction of the dual-chamber magnetron-sputtering unit. This experience will be valuable to them and to the PV community.

Presently substrate size for the sulfurization process is limited to only 1" x 1" cells. Recently, Siemens Solar Industries (SSI) has agreed to donate a selenization and sulfurization unit, in which large 4" x 4" samples can be selenized and sulfurized.

4. Round Robin AES and SIMS Analysis

Together with NREL and University of Illinois, FSEC has carried out the Round Robin, Auger electron spectroscopy (AES) and secondary ion mass spectroscopy (SIMS) analysis of CIGS and CIGS/CdS samples prepared at the SSI, NREL, and IEC. The results show that SIMS analysis using both cesium and oxygen beams can provide important and useful information. The results are being presented at the National CIS Thin Film Partnership Program Meeting.

5. IxV Characteristics of CdTe Modules and Analysis of CdTe Module Samples

Measurements IxV characteristics of seven CdTe modules from First Solar (formerly Solar Cells Inc) were carried out. Samples extracted from a First Solar (formerly Solar Cells Inc) CdTe module were analyzed by Auger electron spectroscopy, X-ray photoelectron spectroscopy, and energy dispersive X-ray spectroscopy (EDS). These results are being submitted separately to NREL and First Solar.

CIGS2 Thin Film Solar Cells On Stainless Steel Foil

Neelkanth G. Dhere and Shantinath R. Ghongadi
Florida Solar Energy Center
1679 Clearlake Road, Cocoa, FL 32922-5703

ABSTRACT

CuIn_{1-x}Ga_xS₂ (CIGS2) thin-film solar cells are of interest for space power applications because of the near optimum bandgap for AM0 solar radiation in space. CuIn_{1-x}Ga_xSe_{2-y}S_y (CIGS) and CIGS2 solar cells are expected to be superior to Si and GaAs solar cells for the space missions especially in terms of the performance at the end of low earth orbit (LEO) mission. Ultra-lightweight thin-film solar cells deposited on flexible stainless steel (SS) foils have a potential for achieving high specific power.

Magnetron-sputter-deposition parameters of molybdenum back-contact layer were optimized so as to minimize residual stress. Cu-rich Cu-Ga/In layers were sputter-deposited on unheated Mo-coated SS foils from CuGa(22%) and In targets. Well-adherent, large (3 μm), compact-grain Cu-rich CIGS2 films were obtained by sulfurization in a Ar:H₂S 1:0.04 mixture and argon flow rate of 650 sccm, at the maximum temperature of 475° C for 60 minutes with intermediate 30 minute annealing step at 120° C. p-type CIGS2 thin films were obtained by etching away the Cu-rich layer segregated at the surface in a dilute KCN solution. XRD analysis of a CIGS2 film on SS foil revealed growth of chalcopyrite CIGS2 phase having $a_0 = 5.519 \text{ \AA}$ and $c_0 = 11.125 \text{ \AA}$ and {112} preferred orientation. Positive SIMS depth profile of CIGS2 film showed gallium concentration increasing toward the back contact.

Solar cells were completed by deposition of CdS heterojunction partner layer by chemical bath deposition, transparent-conducting ZnO/ZnO:Al window bilayer by RF sputtering, and vacuum deposition of Ni/Al contact fingers through metal mask. PV parameters of a CIGS2 solar cell on SS flexible foil measured under AM 0 conditions at the NASA GRC were: $V_{oc} = 802.9 \text{ mV}$, $J_{sc} = 25.07 \text{ mA/cm}^2$, $FF = 60.06\%$, and $\eta = 8.84\%$. For this cell, AM 1.5 PV parameters measured at NREL were: $V_{oc} = 788 \text{ mV}$, $J_{sc} = 19.78 \text{ mA/cm}^2$, $FF = 59.44\%$, $\eta = 9.26\%$. Quantum efficiency curve showed a sharp QE cutoff equivalent to CIGS2 bandgap of ~1.50 eV, fairly close to the optimum value for efficient AM0 PV conversion in the space.

INTRODUCTION

CuIn_{1-x}Ga_xS₂ (CIGS2) thin-film solar cells are of interest for space power applications because of the near optimum bandgap for AM0 solar radiation in space [1,2]. Ultra-lightweight thin-film solar cells deposited on flexible stainless steel (SS) foils have a potential for achieving high specific power.

Future space missions would include very large and very small satellites [3]. Solar power satellites were proposed in 1969 [4]. NASA and the Department of Energy have studied options of providing a reference system consisting of two 5-GW satellites. Some long-term plans envisage swarms of distributed, autonomous, small satellites termed microsats or even nanosats

to perform specific tasks [3]. Some missions will use solar electric propulsion (SEP) instead of rockets [5]. This technology has been successfully demonstrated in Deep Space I.

CIGS2 thin film solar cells may be able to reduce both the manufacturing cost and the mass per unit power by an order of magnitude from the current levels. The thin-film technology could conservatively reduce the array-manufacturing cost of medium-sized five-kilowatt satellite from the current level of \$2000,000 to less than \$500,000 [6]. For small satellites, increasing the solar array specific power from a currently typical value of 65 Wkg^{-1} will allow for either an increase in payload power or payload mass, or both. Weight benefits of higher efficiency cells are decreased and high costs become less affordable in the case of flexible thin-film blanket arrays that can be easily rolled out [5]. Non-rigid cells also have an advantage in stability. Polymer substrates, appealing for their strength, weight, and ease of processing, have not yet demonstrate long-term survivability in space environment which includes repeated thermal stresses, radiation, and atomic oxygen. Because of the low initial velocities and steady acceleration, SEP satellites must spend long periods in intense regions of trapped radiation belts. $\text{CuIn}_{1-x}\text{Ga}_x\text{Se}_{2-y}\text{S}_y$ (CIGS) and CIGS2 solar cells are expected to be superior to Si and GaAs solar cells for the space missions especially in terms of the performance at the end of low earth orbit (LEO) mission [7,8]. The potential for improved radiation resistance of thin-film solar cells relative to single-crystal cells, could extend the mission lifetimes substantially. Recent studies have shown that 12.6% efficient thin film cells would start to become cost-competitive in GEO and LEO missions [5]. However, significant technological hurdles remain before thin-film technology could be implemented as the primary power source for spacecraft. This paper presents research efforts for the development of CIGS2 thin-film solar cells on flexible SS foil substrate for space power.

EXPERIMENTAL TECHNIQUE

DC sputter-deposition parameters of molybdenum back-contact layer from 3" diameter magnetron sputtering source were optimized so as to minimize the residual stresses developed during deposition. Depending on the working gas pressure, residual stresses can develop in refractory metal thin films prepared by magnetron sputtering. Films deposited below a transition pressure are in compression whereas those deposited above the transition pressure develop tensile stress [9]. It is believed that such stress reversal is dependent on energetic bombardment by reflected neutrals and/or sputtered atoms. At relatively low pressures, the arriving atoms have higher kinetic energy and the resulting film has dense microstructure but at the same time experience compressive stress. A higher working gas pressure is expected to moderate the flux and energy of these particles and consequently form a more open morphology with tensile stress. The adhesive strength at the Mo/ Stainless Steel Substrate was tested using a simple scotch tape test to gauge tendency of the films to peel off due to excessive residual stresses. Sheet resistance was measured with two-probe resistance measurement. Composite Mo back contact films prepared by alternatively depositing three layers at high argon pressure of 9 mTorr and low power of 40 W, and three layers deposited at low argon pressure on 5 mTorr and high power of 70 W demonstrated good adhesion and very low sheet resistance.

Approximately 40%-Cu-rich Cu-Ga/In layers were sputter-deposited on unheated Mo-coated SS foils from CuGa(22%) and In targets. Well-adherent, large-grain Cu-rich CIGS2 films were obtained by sulfurization in a $\text{Ar:H}_2\text{S}$ 1:0.04 mixture and argon flow rate of 650 sccm, at the maximum temperature of 475°C for 60 minutes with intermediate 30 minute annealing step at

120° C. p-type CIGS2 thin films were obtained by etching away the Cu-rich layer segregated at the surface in dilute KCN solution.

The chemical composition of CIGS2 films was analyzed by electron-probe microanalysis (EPMA) and secondary ion mass spectrometry (SIMS) depth profiling by positive SIMS using CAMECA IMS-3F system with oxygen primary beam current of 150 nA, impact energy of 5.5 keV, angle of incidence of 42°, rastered over a 250 μm x 250 μm area, with source at 10 keV and sample at 4.5 keV. Structure and morphology of CIGS2 films was studied by x-ray diffraction (XRD) and scanning electron microscopy (SEM).

Solar cells were completed by deposition of CdS heterojunction partner layer by chemical bath deposition, transparent-conducting ZnO/ZnO:Al window bilayer by RF sputtering, and vacuum deposition of Ni/Al contact fingers through metal mask. PV parameters of a solar cell on SS foil were measured under AM 1.5 and AM 0 illumination respectively at National Renewable Energy Laboratory (NREL) and NASA Glenn Research Center (NASA GRC).

RESULTS AND DISCUSSION

Once the Cu-excess in CIGS2 films was optimized, very uniform, bluish gray CIGS thin films were obtained on flexible SS foils. The two probe method showed very low resistance indicating that the film was copper rich and Cu_{2-x}S phase has segregated uniformly on the surface.

Average atomic concentrations of Cu:In:Ga:S proportion of 24.83:22.96:2.07:50.14 measured by EPMA in CIGS2 films on SS foils at incident electron beam energy of 20 keV. This is equivalent to CIGS2 compound formula of $\text{Cu}_{0.99}\text{In}_{0.92}\text{Ga}_{0.08}\text{S}_2$. At incident electron beam energy of 10 keV, the proportion of gallium was lower due to the tendency of gallium to diffuse towards the back contact. In an unetched Cu-rich CIGS2 film, proportion of atomic concentration of Cu:In:Ga:S as measured by EPMA at 20 keV was 41.55:13.41:1.09:43.963.

SIMS depth profile for the etched sample showed uniform sulfur signal throughout the entire thickness (Figure 1). Gallium signal strength increased slightly while indium signal strength decreased at larger depths. The increase in copper signal strength at higher depths was probably an artifact of film roughness. Potassium incorporation in the film was due to etching with KCN solution. Sodium was not intentionally added and also the samples were handled with extreme care using tweezers. Even then small amounts of sodium were detected in the film.

SEM image of an unetched CIGS2 thin film on SS foil substrates showed large (~3 μm size), compactly packed, faceted grains (Figure 2). Besides the 110 peak from molybdenum, XRD pattern for the etched CIGS2 film on SS foil showed the following reflections from the chalcopyrite CIGS2 phase with $a_0 = 5.519 \text{ \AA}$ and $c_0 = 11.125 \text{ \AA}$: 101, 112, 103, 200, 211, 220, 213, 312, 322, 400, and 332 (Figure 3). Reflection 112 was the strongest. Thus the CIGS2 film grew with {112} preferred orientation.

PV parameters of a CIGS2 solar cell on SS flexible foil measured under AM 0 conditions at the NASA GRC were as follows: $V_{oc} = 802.9 \text{ mV}$, $J_{sc} = 25.07 \text{ mA/cm}^2$, $FF = 60.06\%$, and $\eta = 8.84\%$ (Figure 4). For this cell, AM 1.5 PV parameters measured at NREL were as follows: $V_{oc} = 788 \text{ mV}$, $J_{sc} = 19.78 \text{ mA/cm}^2$, $FF = 59.44\%$, $\eta = 9.26\%$. Variation of quantum efficiency (QE) with photon energy curve showed a sharp QE cutoff at photon energy equivalent to CIGS2 bandgap of ~1.50 eV. This is fairly close to the required optimum value for efficient AM0 PV conversion in the space.

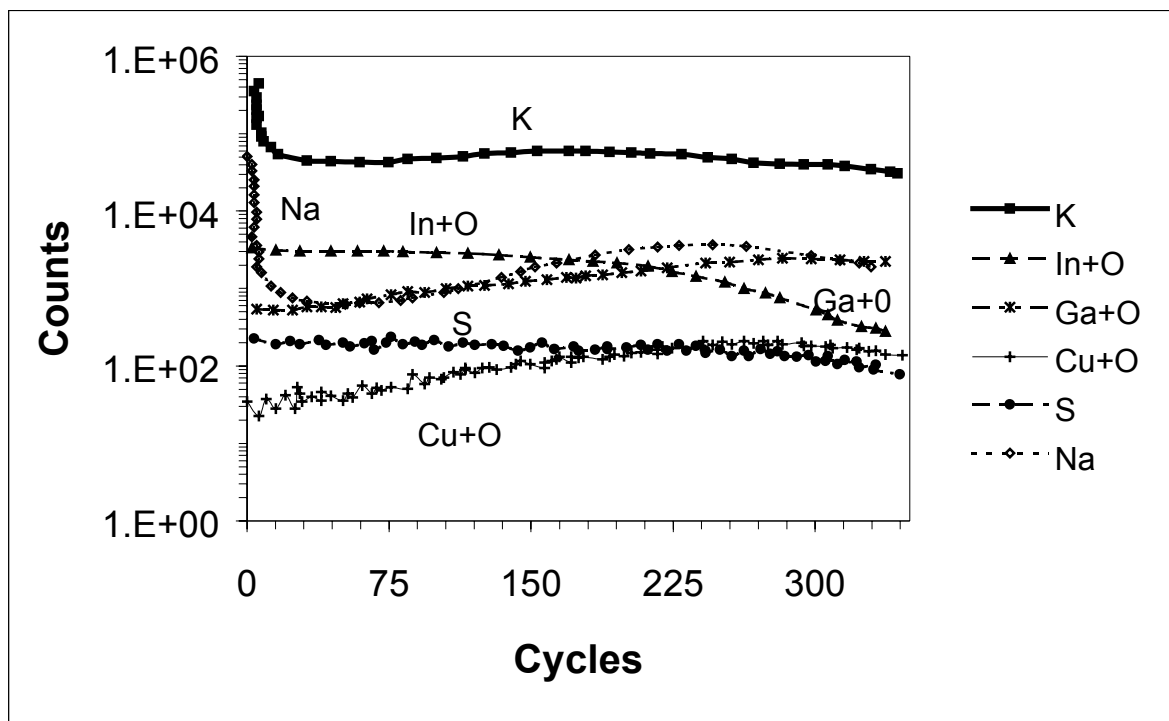


Fig. 1. SIMS analysis of CIGS2 thin film on SS foil.

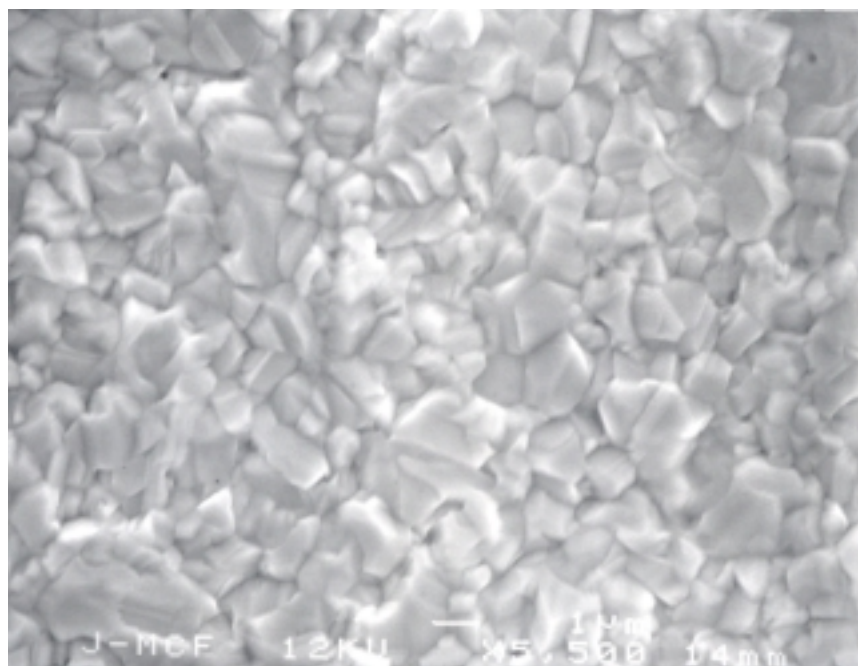


Fig. 2. SEM image of CIGS2 thin film on SS foil.

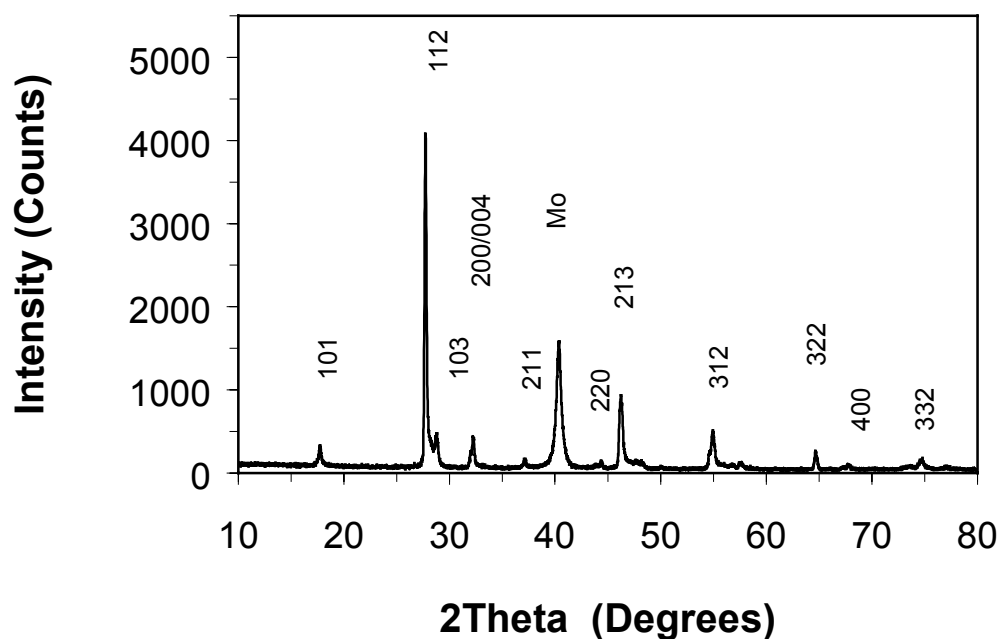


Figure 3. XRD pattern of CIGS2 film on SS foil with 112 preferred orientation.

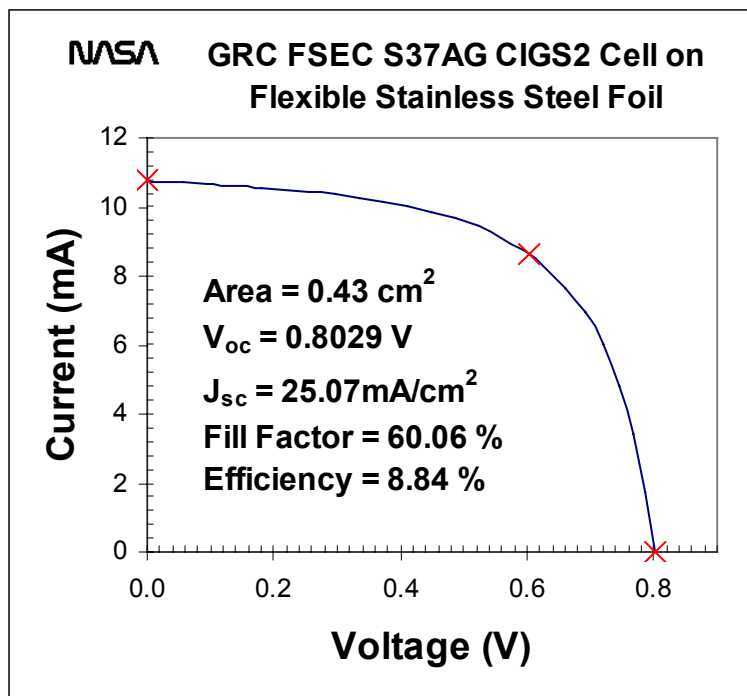


Figure 4. AM1.5 I-V characteristic of CIGS2 thin film solar cell on SS foil.

CONCLUSIONS

CIGS2 thin films having composition of $\text{Cu}_{0.99}\text{In}_{0.92}\text{Ga}_{0.08}\text{S}_2$ were prepared on flexible SS substrates. The films consisted of large ($\sim 3\ \mu\text{m}$), compactly-packed, faceted grains and $\{112\}$ preferred orientation of chalcopyrite CIGS2 phase with $a_0 = 5.519\ \text{\AA}$ and $c_0 = 11.125\ \text{\AA}$. PV parameters of a CIGS2 solar cell on SS flexible foil measured under AM 0 conditions were: $V_{oc} = 802.9\ \text{mV}$, $J_{sc} = 25.07\ \text{mA/cm}^2$, $\text{FF} = 60.06\%$, and $\eta = 8.84\%$. For this cell, AM 1.5 PV parameters were: $V_{oc} = 788\ \text{mV}$, $J_{sc} = 19.78\ \text{mA/cm}^2$, $\text{FF} = 59.44\%$, $\eta = 9.26\%$. Quantum efficiency curve showed a sharp QE cutoff equivalent to CIGS2 bandgap of $\sim 1.50\ \text{eV}$, fairly close to the optimum value for efficient AM0 PV conversion in the space.

ACKNOWLEDGEMENTS

This work was supported by the Air Force Research Lab through Jackson and Tull and by the NASA Glenn Research Center. The authors are thankful to Dr. Kannan Ramnathan and Tom Moriarty of NREL for help with Ni/Al contact deposition and AM1.5 measurements respectively, Fred A. Stevie of Agere Systems for help with SIMS analysis, David Scheiman of Ohio Aerospace Institute, NASA GRC for AMO measurements, and Dr. Subhendu Guha of United Solar Systems Corp for supplying SS sheets.

REFERENCES

1. S. G. Bailey and D. J. Flood, *Prog. Photovolt. Res. Appl.* **6**, 1-14, (1998).
2. N. G. Dhere and S. R. Ghongadi, *Proc. 28th IEEE Photovoltaic Specialists Conference*, Anchorage, Alaska, (2000).
3. P. A. Iles, *Solar Energy Materials and Solar Cells* **68**, 1-13, (2001).
4. P. E. Glaser, G. M. Hanley, R. H. Nansen, and R. L. Kline, *IEEE Spectrum*, pp. 52-58 (May 1979).
5. E. L. Ralph, and T. W. Woike, *Proceedings of 37th American Institute of Aeronautics and Astronautics Aerospace Sciences Meeting and Exhibit* pp. 1-7 (1999).
6. J. Tringe, J. Merrill, and K. Reinhardt, *Proc. 28th IEEE Photovoltaic Specialists Conference*, Anchorage, Alaska, (2000).
7. S. Messenger, R. Walters, G. Summers, T. Morton, G. La Roche, C. Signorini, O. Anzawa, and S. Matsuda, *Proc. 16th European Photovoltaic Solar Energy Conference*, Glasgow, UK, (2000).
8. A. Boden, D. Bräunig, J. Klaer, F. H. Karg, B. Hösselbarth, G. La Roche, *Proc. 28th IEEE Photovoltaic Specialists Conference*, Anchorage, Alaska, (2000).
9. J. A. Thornton, J. Tabock, and D. W. Hoffman, *Thin Solid Films* **64**, 111-119, (1979).

Large-Area, Dual-Chamber Magnetron-Sputtering Unit for Preparation of CIGS Thin Film Solar Cells

Neelkanth G. Dhere, Shantinath R. Ghongadi, Anant H. Jahagirdar, Mandar B. Pandit, and Ankur A. Kadam
Florida Solar energy Center
1679 Clearlake Road, Cocoa, FL 32922-5703

ABSTRACT

CuIn_{1-x}Ga_xS₂ (CIGS2) thin film solar cell samples are being prepared routinely on sodalime glass substrates and on metallic foils. PV parameters of a CIGS2 solar cell on SS flexible foil measured under AM 1.5 conditions at NREL were: $V_{oc} = 788$ mV, $J_{sc} = 19.78$ mA/cm², FF = 59.44%, $\eta = 9.26\%$. For this cell, AM 0 PV parameters measured at the NASA GRC were: $V_{oc} = 802.9$ mV, $J_{sc} = 25.07$ mA/cm², FF = 60.06%, and $\eta = 8.84\%$. A large-area, dual-chamber magnetron-sputtering unit has been fabricated. Three 4" x 12" DC magnetron sputtering sources have been installed in the larger chamber for Mo, CuGa, and In sputter deposition. Two 4" x 12" RF magnetron sputtering sources have been installed in the smaller chamber for ZnO and ZnO:Al bilayer window deposition. Selenization and sulfurization of 4" x 4" samples is planned using a furnace being donated by the Siemens Solar ind.

1. Introduction

CuIn_{1-x}Ga_xS₂ (CIGS2) thin-film solar cells are of interest for photovoltaic conversion because of the near optimum bandgap of 1.5 eV [1]. CIGS2 thin films prepared with gallium content x of 0.31 and 0.36 have been found to have a bandgap of 1.71 eV and 1.76 eV respectively [2]. Recently, large-grain CIGS2 films with Ga content x in the range 0.4 to 0.5 have been prepared [3]. Such films will be suitable for fabrication of the front cell in a tandem structure. FSEC PV Materials Laboratory has facilities for magnetron sputter deposition of molybdenum back contact layer and CuGa/In metallic precursor layers, selenization and sulfurization of metallic precursors, CdS chemical bath deposition and ZnO/ZnO:Al RF sputter deposition. Earlier, the substrate size was limited to 1" x 1". A large-area, dual-chamber magnetron-sputtering unit has been fabricated recently. The chambers are equipped with cryopumps, two-stage mechanical vacuum pumps, throttled-gate valves, mass-flow controllers for argon and oxygen, and convectron and Bayard-Alpert ionization gauges. A large number of feed-thru ports have been provided to both the chambers for rotation and electrical feed-thru's. This will permit addition of *in situ* diagnostic tools.

The large chamber (Fig. 1) has three 4" x 12" DC magnetron sputtering sources, installed for sputter deposition from molybdenum, indium, and copper, CuGa (22%) or CuGa (67%) targets. A linear substrate movement set-up has been fabricated for "in line" deposition of molybdenum back contact and Cu-Ga/In metallic precursors. Presently the movement of the substrates is done

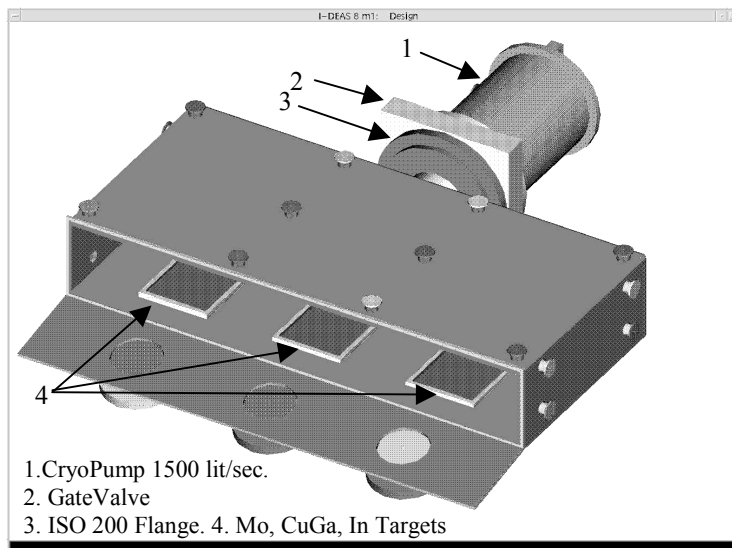


Fig. 1: Large chamber with three sputtering targets, Gate valve and Cryo Pump (1500 lit/sec).

manually. Precise movement using stepper motor will be done in the near future.

The small chamber (Fig. 2) has two 4" x 12" RF magnetron sputtering sources, installed for RF sputter deposition from ZnO and ZnO:Al targets.

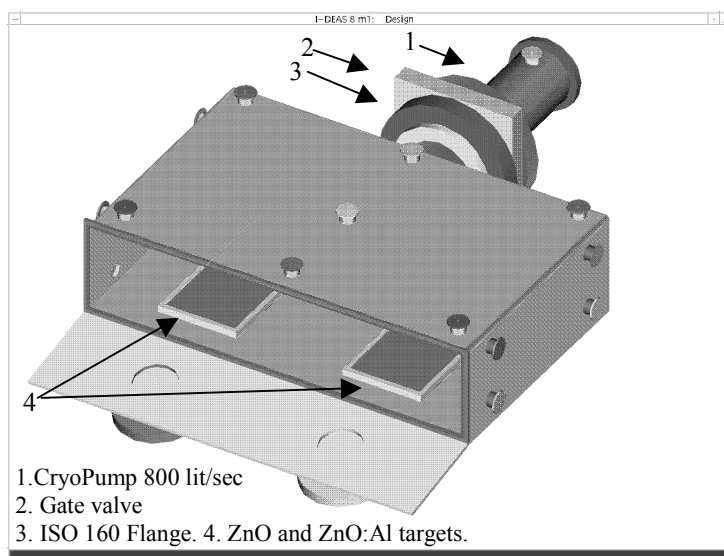


Fig. 2: Small Chamber with ZnO and ZnO:Al targets, Gate Valve and Cryo Pump (800 lit/sec)

The thickness uniformity along the 12" dimension is expected to be better than $\pm 2\%$ over the center width of 5" and better than $\pm 3\%$ over the center width of 6" for linear substrates motion along the 4" dimension. Moreover, the sputtering sources are expected to provide excellent ($>40\%$) target utilization. A four-hearth e-beam source has also been procured for vacuum evaporation of Ni/Al contact grids. The vacuum chambers were designed at FSEC and were built elsewhere based on FSEC design. The complete system was designed and constructed at FSEC. Several Graduate students have been trained in the design and construction of the dual-chamber magnetron-sputtering unit. This experience will be valuable to them and to the PV community.

2. Experimental Technique

The routine experimental technique in fabricating CIGS2 thin film solar cells at FSEC consists of two stages. First stage is the sputter deposition of Cu+Ga and In on Mo coated glass substrates or SS foils. This stacked elemental layer is sulfurized in H_2S : Ar gas environment using a three-zone furnace. The Cu-rich stoichiometry during the growth of CIGS2 films results in an improved morphology, i.e. enhanced grain sizes of the polycrystalline films. Presently we have the limitation in sulfurization process for only 1" x 1" cells. Recently, Siemens Solar Industries (SSI) has agreed to donate a selenization and sulfurization unit, in which large 4" x 4" samples can be selenized and sulfurized. The copper rich Cu_xS phase, precipitating at the top during sulfurization is etched using 10% KCN. This is followed by deposition of CdS buffer layer by chemical bath deposition (CBD) and ZnO window layer. Presently the chemical bath deposition is limited to 1" x 1" samples but we have plans for the fabrication of new CBD CdS facility both for large area (4" x 4") solar cells. Also presently the deposition of ZnO and ZnO:Al is also limited to one 1" x 1" sample per run. However, with fabrication of the large-Area, inline chamber (Fig. 2), we will be able to sputter deposit more samples in a single run.

3. Round Robin AES and SIMS Analysis

Together with NREL and University of Illinois, FSEC has carried out the round robin, Auger electron spectroscopy (AES) and secondary ion mass spectroscopy (SIMS) analysis of CIGS and CIGS/CdS samples prepared at the SSI, NREL, and Institute of Energy Conversion. The results show that SIMS analysis using both oxygen and cesium beams can provide important and useful information. The results are being presented at the National CIS Thin Film Partnership Program Meeting.

4. IxV characteristics of CdTe modules

Measurements of IxV characteristics of seven CdTe modules from First Solar (formerly Solar Cells Inc) have been carried out periodically. The results have been submitted to NREL and First Solar.

5. Results and Discussion

X-ray diffraction (XRD) pattern of the as-deposited (Cu+Ga)/In metallic precursors indicated the presence of

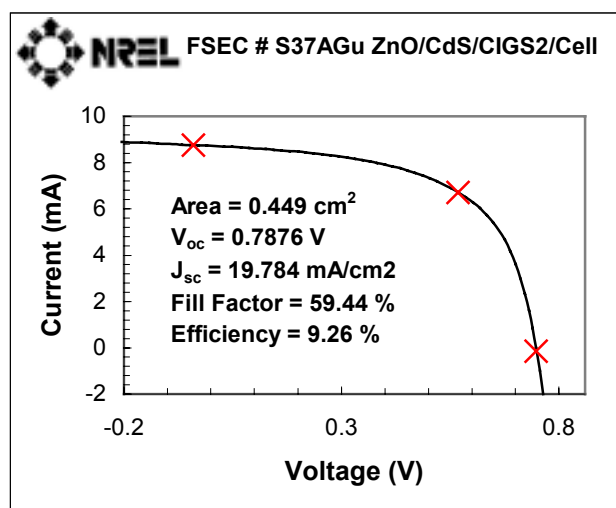


Fig. 3. I - V curve of CIGS2 thin film solar cell on SS foil.

highly oriented $\text{Cu}_{11}\text{In}_9$ phase without any elemental or alloy phases. XRD pattern of near stoichiometric, slightly Cu-poor, etched CIGS2 thin film showed a (112) texture growth of chalcopyrite $\text{CuIn}_{0.7}\text{Ga}_{0.3}\text{S}_2$ phase with $a = 5.67 \text{ \AA}$ and $c = 11.34 \text{ \AA}$ [4]. PV parameters of a CIGS2 solar cell on 127 μm thick SS flexible foil measured at NREL under AM 1.5 conditions were: $V_{oc} = 788 \text{ mV}$, $J_{sc} = 19.78 \text{ mA/cm}^2$, $FF = 59.44\%$, $\eta = 9.26\%$ (Fig. 3). For this cell, AM 0 PV parameters measured at the NASA GRC were: $V_{oc} = 802.9 \text{ mV}$, $J_{sc} = 25.07 \text{ mA/cm}^2$, $FF = 60.06\%$, and efficiency $\eta = 8.84\%$ [4].

6. Acknowledgements

This work was supported by the National Renewable Energy Laboratory, through the contract XAK-8-17619-12. The authors are thankful to Dr. Kannan Ramnathan and Tom Moriarty of NREL for help with Ni/Al contact deposition and AM 1.5 measurements respectively and Fred A. Stevie of Agere Systems for help with SIMS analysis.

REFERENCES

- [1] N. G. Dhere, S. R. Kulkarni and P. K. Johnson, Bandgap Optimization of CIGS2 Space Solar Cells, Proc. 16th European Photovoltaic Solar Energy Conference, Glasgow, UK, 978, (2000).
- [2] N. G. Dhere, J. A. Turner, A. M. Fernandez, H. Mametsuka and E. Suzuki, Photoelectrochemical Characterization of High-Ga Content CIGS2 Thin Films, 52nd Meeting Abstracts Int Soc Electrochemistry, San Francisco, CA, Sept. 2-7, 2001, # 1117.
- [3] N. G. Dhere, S. R. Kulkarni and S. R. Ghongadi, "PV Characterization of CIGS2 Thin Film Solar Cells", Proc. 28th IEEE Photovoltaic Specialists' Conference, Anchorage, Alaska, Sept. 15-22, 1046, (2000).
- [4] N. G. Dhere, S. R. Ghongadi, M. B. Pandit, A. H. Jahagirdar and D. Scheiman, CIGS2 Thin-Film Solar Cells On Flexible Foils For Space Power, Proc. 17th Space PV Res and Technol (SPRAT) Conf., Cleveland, OH, Sept. 11-13, 2001.

LIGHTWEIGHT CIGS2 THIN-FILM SOLAR CELLS ON STAINLESS STEEL FOIL

Neelkanth G. Dhere, Shantinath R. Ghongadi and Mandar B. Pandit

Florida Solar Energy Center

1679 Clearlake Road, Cocoa, FL 32922-5703, USA

Phone: (407) 638-1442, Fax: (407) 638-1010, e-mail: dhere@fsec.ucf.edu

ABSTRACT: AM 0 PV parameters of large-grain, {112} orientated chalcopyrite CIGS2 thin films solar cells on 127 μm thick SS flexible foil for space power were: $V_{oc} = 802.9 \text{ mV}$, $J_{sc} = 25.07 \text{ mA/cm}^2$, $FF = 60.06\%$, and efficiency $\eta = 8.84\%$. Detailed current versus voltage analysis gave values of series resistance R_s , shunt resistance R_p , diode factor A , and reverse saturation current J_0 of $\sim 0.1 \Omega \text{ cm}^2$, $\sim 600 \Omega \text{ cm}^2$, ~ 2.2 and $\sim 1.85 \times 10^{-8} \text{ A cm}^2$ respectively. A sharp QE cutoff was observed at CIGS2 bandgap of $\sim 1.50 \text{ eV}$. Higher foil roughness resulted in a preliminary low 4.06% (AM 1.5) efficiency of CIGS2 solar cell on 20 μm thick SS foil. Present specific power of 65 W/kg can be increased by over 10 times with 10% AM 0 CIGS cells on 20-25 μm thick SS or Ti foils.

Keywords: CIGS2 solar cells- 1: SS Foil - 2: Light weight

1. INTRODUCTION

The purpose of this research is to develop $\text{CuIn}_{1-x}\text{Ga}_x\text{S}_2$ (CIGS2) thin-film solar cells on flexible stainless steel (SS) foils for space power. CIGS2 thin-film solar cells are of interest for space power applications because of the near optimum bandgap for AM0 solar radiation in space [1-7]. $\text{CuIn}_{1-x}\text{Ga}_x\text{Se}_{2-y}\text{S}_y$ (CIGS) and CIGS2 solar cells are expected to be superior to Si and GaAs solar cells for space missions especially in terms of the performance at the end of low earth orbit (LEO) missions [8,9]. CIGS2 thin film solar cells on flexible SS may be able to increase the specific power by an order of magnitude from the current level of 65 Wkg^{-1} . Thin-film technology could conservatively reduce the array-manufacturing cost of medium-sized five-kilowatt satellite from the current level of \$2000k to less than \$500k [10]. Preparation and properties of CIGS thin-film solar cells deposited on glass substrates have been described in earlier studies [11,12]. This paper presents preparation and detailed photovoltaic (PV) characterization of CIGS2 thin-film solar cells on SS flexible foil substrates for ultra-lightweight space solar power.

2. EXPERIMENTAL TECHNIQUE

DC-magnetron-sputtering parameters for deposition of molybdenum back-contact layer were optimized so as to minimize the residual stresses developed during deposition. Bright annealed stainless steel foils of thicknesses 127 μm and 20 μm were evaluated as possible substrate materials for polycrystalline CIGS2 solar cell. Crystalline phases, surface morphology, and composition-depth profile of CIGS2 films deposited on SS flexible foils substrates were studied by X-ray diffraction (XRD) and scanning electron microscopy (SEM).

Approximately 40%-Cu-rich Cu-Ga/In layers were sputter-deposited on unheated Mo-coated SS foils from

CuGa(22%) and In targets. Well-adherent, large-grain Cu-rich CIGS2 films were obtained by sulfurization in an $\text{Ar:H}_2\text{S}$ 1:0.04 mixture at argon flow rate of 650 sccm and the maximum temperature of 475°C for 60 minutes with intermediate 30 minute annealing step at 135°C . p-type CIGS2 thin films were obtained by etching away the Cu-rich layer segregated at the surface in dilute (10%) KCN solution for 3 minutes [13,14]. Solar cells were completed by deposition of CdS heterojunction partner layer by chemical bath deposition, transparent-conducting ZnO/ZnO:Al window bilayer by RF sputtering, and vacuum deposition of Ni/Al contact fingers through metal mask [15]. PV parameters of the best solar cell on SS foil were measured under AM 0 and AM 1.5 conditions at the NASA Glenn Research Center (GRC) and Natioanl Renewable Energy Laboratory respectively. Detailed PV characteristics were obtained at the Institute of Energy Conversion (IEC) [6,11].

3. RESULTS AND DISCUSSIONS

Surface roughness of SS foil substrates was measured using DEKTAK³ surface profile measuring system. In case of 127 μm thick SS foil, the average roughness (R_a) was 62.3 \AA and average waviness (W_a) was 141.6 \AA . The average roughness and average surface waviness were respectively 396.4 \AA and 773.2 \AA for the 20 μm thick SS foil. XRD and SEM analysis of a CIGS2 film on SS foil revealed growth of large ($\sim 3 \mu\text{m}$), compactly-packed, faceted grains of chalcopyrite CIGS2 phase having $a_0 = 5.519 \text{ X}$ and $c_0 = 11.125 \text{ X}$ and {112} preferred orientation. SIMS depth profile of CIGS2 film showed gallium concentration increasing toward the back contact.

PV parameters of the best CIGS2 solar cell on 127 μm thick SS flexible foil measured under AM 0 conditions at

the NASA Glenn Research Center were: $V_{oc} = 802.9$ mV, $J_{sc} = 25.07$ mA/cm², FF = 60.06%, and $\eta = 8.84\%$. For this cell, AM 1.5 PV parameters measured at NREL were: $V_{oc} = 788$ mV, $J_{sc} = 19.78$ mA/cm², FF = 59.44%, $\eta = 9.26\%$.

Results of the detailed PV characteristics consisting of the analysis of short circuit current, J versus voltage, V and quantum efficiency data obtained at IEC for this cell are presented in the following. The J - V characteristics in light and dark were compared to verify if the light characteristic was essentially a translated curve with light short circuit current, J_{sc} or J_L (Figure 1). There was slight crossover at current densities over $1.9 \times J_{sc}$ indicating a moderately photoconducting heterojunction partner layer.

J - V characteristics under illumination provided J_{sc} , V_{oc} , FF, and 0 , in addition to R_s , R_p . Ascending and descending curves showed hysteresis. The main part of $\log(J+J_{sc})$ versus V_t curves showed diode behavior (Figure 2). The offset between dark and light curves is attributed to the higher reverse saturation current, J_0 under illumination. The curve is affected by the shunt resistance, R_p at low voltages. In the present cell, shunting effects became predominant below 0.1 mA cm⁻². Usually, slopes are modified due to series resistance at very high currents. In the present case, series resistance effect was not observed even at ~ 59 mA cm⁻² i.e. $\sim 3 \times J_{sc}$.

The dJ/dV versus V curve measures ac conductance around J_{sc} (Figure 3). For the dark curve, it gave a reasonable value of 600Ω cm² for the shunt resistance, R_p . The light curve showed a slight change of collection with voltage. The un-smoothed light curve was noisy due to flicker in xenon arc lamp. The scatter was reduced by using values of dJ/dV calculated by the nine-point differential method. dV/dJ versus $1/J+J_{sc}$ curve was plotted

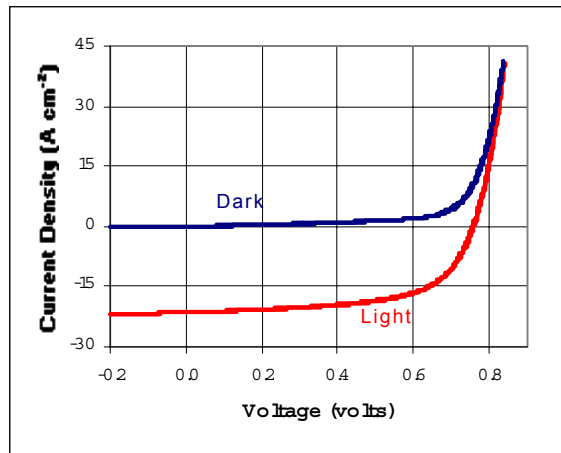


Fig. 1. Variation of light and dark current densities with voltage

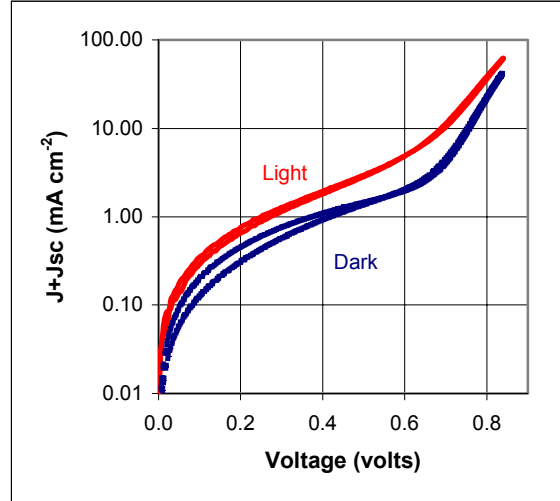


Fig. 2. $\log(J+J_{sc})$ versus total voltage V_t curves

to estimate ac resistance in forward bias. The straight lines show diode or exponential behavior (Figure 4). The intercept at ∞ current gave a very low value of series resistance, R_s of $\sim 0.1 \Omega$ cm². It can be seen that there is moderate hysteresis. It indicates non-coincidence between ascending and descending curves. Values of the diode factor, A and reverse saturation current density, J_0 can be obtained from a plot of natural logarithm of $(J+J_{sc})$ versus corrected voltage V' i.e. $(V-R_sJ)$. Figure 5 shows a plot of the diode factor, A and reverse saturation current,

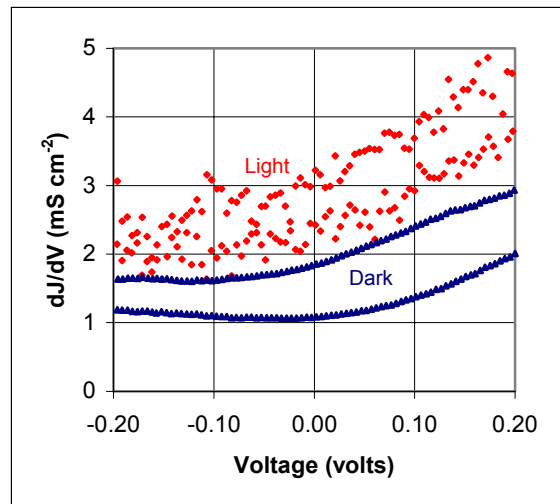
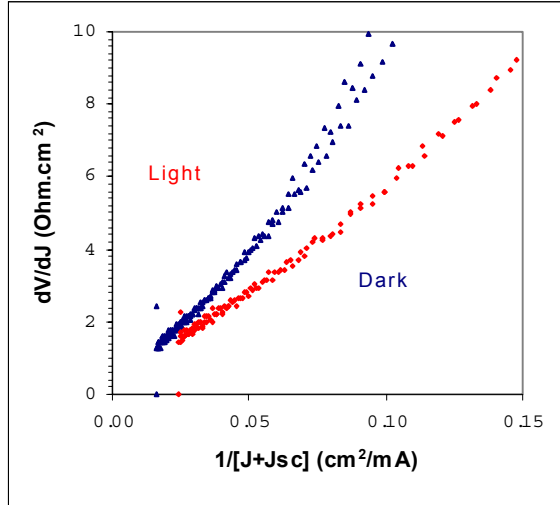


Fig. 3. dJ/dV versus voltage characteristics

Fig. 4. Variation of dV/dJ with $1/[J+J_{sc}]$

J_0 versus $\ln J$ (dark). Values of diode factor, A and reverse saturation current, J_0 can be seen to vary respectively around ~ 2.21 and $\sim 1.85 \times 10^{-8} \text{ A cm}^{-2}$ over a wide range of current densities.

Quantum efficiency (QE) curves were obtained in the dark and under AM1 light illumination, without bias ($V = 0$) and with reverse (-0.5 V) and forward (0.5 V) bias (Figure 6). They showed only a modest loss at high energy by the thin heterojunction partner CdS layer.

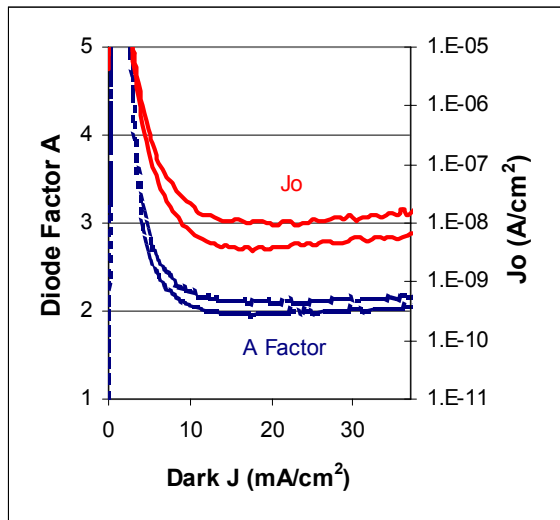
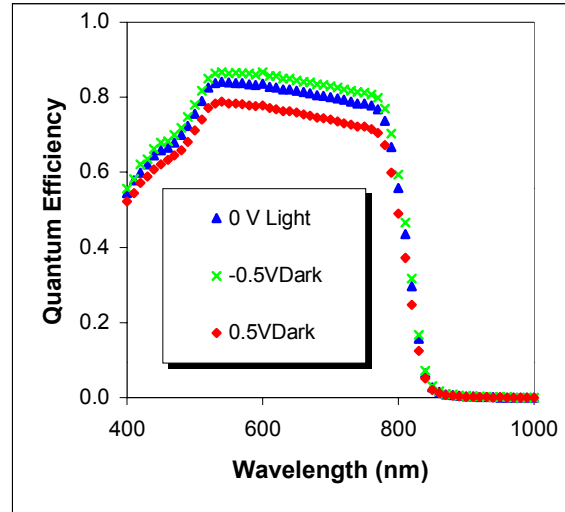
Fig. 5. Variation of diode factor, A , and reverse saturation current density, J_0 , with the dark current density, J .

Fig. 6. Variation of quantum efficiency with wavelength.

At low energy, a sharp QE cutoff was observed equivalent to CIGS2 bandgap of $\sim 1.50 \text{ eV}$.

Another set of curves was obtained for normalized QE versus photon energy in electron-volt, eV. For this purpose, the peak value of each curve was normalized to 1. At low energies, the curves showed almost no difference in collection and a QE cut off at $\sim 1.50 \text{ eV}$. Unbiased samples showed CdS absorption at high energies. Detailed PV characterization consisting of the analysis of short circuit current, J versus voltage, V and quantum efficiency data showed that CIGS2 thin film solar cells on SS substrates were normal without serious limitations and with promising characteristics.

Preliminary experiments were carried out for preparation of CIGS2 solar cells on $20 \mu\text{m}$ thick SS and $25.4 \mu\text{m}$ thick titanium foils. PV parameters of an un-optimized cell fabricated on $20 \mu\text{m}$ thick SS foil and measured at NREL under AM 1.5 conditions were: $V_{oc} = 740 \text{ mV}$, $J_{sc} = 13.129 \text{ mA/cm}^2$, $FF = 41.63\%$, efficiency $\eta = 4.06\%$. It may be noted that the average roughness (R_a) of $20 \mu\text{m}$ thick SS foil was 396.4 \AA while that of $127 \mu\text{m}$ was 62.3 \AA . The loss of efficiency is attributed to surface roughness. It is expected that when smoother $20 \mu\text{m}$ SS foil become available, it would be possible to prepare CIGS2 or CIGS solar cells with AM 0 efficiency in the range of 10 to 15%. Table I provides the projected specific power in W/Kg of flexible metallic substrate for 10 and 15% AM 0 efficient CIGS2 solar cells. Thus it can easily be seen that even 10% AM 0 CIGS cells on thin SS or Ti foils will increase the specific power by over an order of magnitude from the present value of 65 W/kg [16].

Table I. Projected Specific Power in W/Kg.

Substrate Thickness Material	Projected Specific Power in W/Kg	
	AM 0 η = 10%	AM 0 η = 15 %.
127- μ m (5 mil) SS foil	133	200
20- μ m (< 1mil) SS foil	769	1153
25.4- μ m (1 mil) Ti foil	1016	1524

5. CONCLUSIONS

Preparation parameters were optimized to obtain large ($\sim 3 \mu\text{m}$), compactly-packed, faceted-grain, CIGS2 thin films on SS flexible foil with {112} preferred orientation of chalcopyrite phase having $a_0 = 5.519 \text{ \AA}$ and $c_0 = 11.125 \text{ \AA}$. AM 0 PV parameters of a CIGS2 solar cell on 127 μm SS flexible foil were: $V_{oc} = 802.9 \text{ mV}$, $J_{sc} = 25.07 \text{ mA/cm}^2$, $FF = 60.06\%$, and $\eta = 8.84\%$. Detailed J-V analysis gave values of series resistance R_s , shunt resistance R_p , diode factor A , and reverse saturation current J_0 , of $\sim 0.1 \Omega \text{ cm}^2$, $\sim 600 \Omega \text{ cm}^2$, ~ 2.2 and $\sim 1.85 \times 10^{-8} \text{ A cm}^{-2}$ respectively. Quantum efficiency curve showed a sharp QE cutoff equivalent to CIGS2 bandgap of $\sim 1.50 \text{ eV}$, fairly close to the optimum value for efficient AM0 PV conversion in the space. Low 4.06% (AM 1.5) efficiency of an un-optimized CIGS2 solar cell on 20 μm thick SS foil is attributed to higher foil roughness. Calculations show that even 10% AM 0 CIGS cells on 20-25 μm thick SS or Ti foils will increase the specific power by over 10 times from the present value of 65 W/kg.

ACKNOWLEDGEMENTS

This work was supported by the National Renewable Energy Laboratory (NREL) and the NASA Glenn Research Center. The authors are thankful to Dr. William A. Shafarman of Institute of Energy Conversion, University of Delaware, for J-V and QE measurements and discussions, David Scheiman of Ohio Aerospace Institute for AMO measurements, and Dr. Kannan Ramnathan of NREL for help with Ni/Al grid deposition and discussions.

REFERENCES

- [1] D. J. Flood, Prog. Photovolt. Res. Appl. **6** (1998) 187-192.
- [2] S. G. Bailey and D. J. Flood, Prog. Photovolt. Res. Appl. **6** (1998) 1-14.
- [3] N. G. Dhere, S. R. Ghongadi, M. B. Pandit, and A. H. Jahagirdar, Proc. 17th NASA Space Power Conference (SPRAT), Cleveland, Ohio, 2001.
- [4] N. G. Dhere and S. R. Ghongadi, Mat. Res. Soc. Symp. Proc. **668** (2001) H3.4.1-H3.4.6.
- [5] N. G. Dhere, S. R. Kulkarni, and P. K. Johnson, Proc. 16th European Photovoltaic Solar Energy Conference, Glasgow, UK, (2000) 978-981.
- [6] N. G. Dhere, S. R. Kulkarni and S. R. Ghongadi, PV characterization of CIGS2 thin film solar cells, 28th IEEE Photovoltaic Specialists Conference, Anchorage, Alaska, (2000) 1046-1049.
- [7] N. G. Dhere, S. R. Kulkarni, S. S. Chavan and S. R. Ghongadi, Proc. NASA Space Power Conference (SPRAT), Cleveland, Ohio, (1999).
- [8] S. Messenger, R. Walters, G. Summers, T. Morton, G. La Roche, C. Signorini, O. Anzawa, and S. Matsuda, Proc. 16th European Photovoltaic Solar Energy Conference, Glasgow, UK, (2000) 974-977.
- [9] A. Boden, D. Bräunig, J. Klaer, F. H. Karg, B. Hösselbarth, G. La Roche, Proc. 28th IEEE Photovoltaic Specialists Conference, Anchorage, Alaska, (2000) 1038-1041.
- [10] J. Tringe, J. Merrill, and K. Reinhardt, Proc. 28th IEEE Photovoltaic Specialists Conference, Anchorage, Alaska, (2000) 1242-1245.
- [11] N. G. Dhere, S. Kuttath, K. W. Lynn, R. W. Birkmire, and W. N. Shafarman, Proc. 1st World Conf. Photovoltaic Solar Energy Conf., Hawaii, (1994) 190-193.
- [12] N. G. Dhere, S. Kuttath, and H. R. Moutinho, J. Vac. Sci. & Technol. A **13** (1995) 1078-1082.
- [13] R. Scheer, Trends in Vac. Sci. & Technol. **2** (1997) 77-112.
- [14] J. Klaer, J. Bruns, R. Henninger, K. Töpper, R. Klenk, K. Ellmer and D. Bräunig, Proc. 2nd World Conf. Photovoltaic Solar Energy Conf., Vienna, (1998) 537-540.
- [15] K. Ramanathan, F. S. Hasoon, H. Al-Thani, J. Alleman, J. Keane, J. Dolan, M. A. Contreras, R. Bhattacharya and R. Noufi, Proc. NCPV Program Rev. Meeting, Lakewood, CO, (2001) 45-48.
- [16] J. R. Tuttle, A. Szalaj and J. Keane, Proc. 28th IEEE Photovoltaic Specialists Conference, Anchorage, Alaska, (2000), 1042-1045.

REPORT DOCUMENTATION PAGE			Form Approved OMB NO. 0704-0188	
Public reporting burden for this collection of information is estimated to average 1 hour per response, including the time for reviewing instructions, searching existing data sources, gathering and maintaining the data needed, and completing and reviewing the collection of information. Send comments regarding this burden estimate or any other aspect of this collection of information, including suggestions for reducing this burden, to Washington Headquarters Services, Directorate for Information Operations and Reports, 1215 Jefferson Davis Highway, Suite 1204, Arlington, VA 22202-4302, and to the Office of Management and Budget, Paperwork Reduction Project (0704-0188), Washington, DC 20503.				
1. AGENCY USE ONLY (Leave blank)		2. REPORT DATE January 2002		3. REPORT TYPE AND DATES COVERED Final Subcontract Report 5 January 1998 – 31 October 2001
4. TITLE AND SUBTITLE CuIn _{1-x} Ga _x Se ₂ Thin Film Solar Cells, Final Subcontract Report, 5 January 1998—31 October 2001				5. FUNDING NUMBERS CF: XAK-8-17619-12 PVP25001
6. AUTHOR(S) N. G. Dhere				
7. PERFORMING ORGANIZATION NAME(S) AND ADDRESS(ES) Florida Solar Energy Center 1679 Clearlake Road Cocoa, FL 32922-5703				8. PERFORMING ORGANIZATION REPORT NUMBER
9. SPONSORING/MONITORING AGENCY NAME(S) AND ADDRESS(ES) National Renewable Energy Laboratory 1617 Cole Blvd. Golden, CO 80401-3393				10. SPONSORING/MONITORING AGENCY REPORT NUMBER NREL/SR-520-31533
11. SUPPLEMENTARY NOTES NREL Technical Monitor: Bolko von Roedern				
12a. DISTRIBUTION/AVAILABILITY STATEMENT National Technical Information Service U.S. Department of Commerce 5285 Port Royal Road Springfield, VA 22161				12b. DISTRIBUTION CODE
13. ABSTRACT (<i>Maximum 200 words</i>) This report describes the development of CIGS ₂ thin-film solar cells on glass and stainless-steel foil substrates; fabrication of a large-area, dual-chamber magnetron-sputtering unit; Round Robin AES and SIMS analysis; and current-voltage characteristics of CdTe modules and analysis of CdTe module samples. More detailed results on CIGS ₂ cells and the large-area, dual-chamber magnetron-sputtering unit were presented at the MRS Conference, the European PV Conference, and NCPV Program Review Meeting and are included in Appendices I, II, and III. The results of Round Robin AES and SIMS analysis were submitted to the National CIGS Team Meeting. The current-voltage characteristics of CdTe modules and results of analyses of CdTe module samples were submitted separately to NREL and First Solar.				
14. SUBJECT TERMS: PV; CIGS ₂ ; thin-film solar cells; magnetron-sputtering unit; stainless-steel foils; electron-probe microanalysis; Auger electron spectroscopy; secondary-ion mass spectroscopy; cesium oxygen beams; X-ray photoelectron spectroscopy; energy-dispersive X-ray spectroscopy				15. NUMBER OF PAGES
				16. PRICE CODE
17. SECURITY CLASSIFICATION OF REPORT Unclassified		18. SECURITY CLASSIFICATION OF THIS PAGE Unclassified		19. SECURITY CLASSIFICATION OF ABSTRACT Unclassified
				20. LIMITATION OF ABSTRACT UL